Scale setting for α_s beyond leading order

K. Hornbostel
Southern Methodist University, Dallas, Texas 75275

G. P. Lepage
Newman Laboratory of Nuclear Studies, Cornell University, Ithaca, New York 14853

C. Morningstar
Carnegie Mellon University, Pittsburgh, Pennsylvania 15213

(Received 26 August 2002; published 27 February 2003)

We present a general procedure for incorporating higher-order information into the scale-setting prescription of Brodsky, Lepage and Mackenzie. In particular, we show how to apply this prescription when the leading coefficient or coefficients in a series in the strong coupling α_s are anomalously small and the original prescription can give an unphysical scale. We give a general method for computing an optimum scale numerically, within dimensional regularization, and in cases when the coefficients of a series are known. We apply it to the heavy quark mass and energy renormalization in lattice NRQCD, and to a variety of known series. Among the latter, we find significant corrections to the scales for the ratio of e^+e^- to hadrons over muons, the ratio of the quark pole to $\overline{\mathrm{MS}}$ mass, the semileptonic B-meson decay width, and the top decay width. Scales for the latter two decay widths, expressed in terms of $\overline{\mathrm{MS}}$ masses, increase by factors of five and thirteen, respectively, substantially reducing the size of radiative corrections.

DOI: 10.1103/PhysRevD.67.034023 PACS number(s): 12.38.Bx, 11.10.Gh, 11.15.Bt, 11.15.Ha

I. INTRODUCTION

QCD processes computed to a finite order in perturbation theory depend on both the choice of renormalization scheme and the scale for the running coupling constant $\alpha_s(q)$. In particular, changes in the scale induce variations at the first neglected order. While these variations diminish as higher orders are included, for low-order calculations they can be significant, particularly for processes sensitive to relatively low scales. Finding an optimum, physically motivated method for choosing this scale in such cases is important not only to produce accurate results, but also to reasonably estimate convergence based on the size of the series terms. Such a method allows a meaningful prediction or comparison with data even at leading order.

A variety of procedures have been proposed to select this scale [1–17]. In this paper, we investigate the prescription of Brodsky, Lepage and Mackenzie (BLM) [4]. In this method, one chooses the scale q^* for $\alpha_s(q^*)$ which approximates the use of the fully dressed gluon propagator within that process. The choice is equivalent to determining the dominant momentum flowing through the propagator within a diagram [13,16]. It has been applied successfully in a large variety of perturbative calculations. Among these, it was essential in demonstrating the viability of lattice perturbation theory [13], and in extracting a precise value of α_s from lattice simulations of the Υ and ψ systems [18,19].

In this paper, we generalize the prescription to remedy an anomaly observed in a variety of applications, particularly apparent when determining the scale over a range of parameters in the action. The nonrelativistic (NRQCD) QCD mass and energy renormalizations presented in Sec. IX B are typical examples. In most of these cases, for some value of the bare quark mass, the BLM scale diverges. We show that this breakdown is not a flaw in the general prescription, but rather the result of employing only a single vacuum-polarization insertion to estimate the typical momentum. While we focus on setting the scale for one-loop diagrams, we use information from two-loop and higher insertions within these diagrams to provide a simple generalization which accurately estimates the scale over the full range of parameters. It is straightforward to implement for both analytic and numerical computations, requiring only a modest extension beyond the leading order determination. For both computations, one obtains the additional information required from one higher moment in $\log(q^2)$ within the same diagram as was used in the lowest order application. For processes where the series coefficients are known, it requires only identifying the coefficient from vacuum polarization at the next order.

We note that other authors have developed a variety of extensions to Ref. [4], which explore conformal symmetry and the relation between various perturbative schemes [9–11], or which estimate nonperturbative contributions and resum classes of diagrams to all orders [14,16]. Our goal is more modest: to provide a simple but robust scale determination for a process calculated to finite order. Specifically, we choose a single optimized scale for the leading, one-loop diagram, to be used for all orders. We show, however, that our prescription should effectively absorb into the leading term or terms the bulk of contributions from all higher order diagrams which dress the leading gluon.

II. GENERAL PRESCRIPTION

Following Refs. [4,13], we choose the V scheme based on the static-quark potential because of the direct connection between the scale of its coupling α_V and the momentum

 ©2003 The American Physical Society

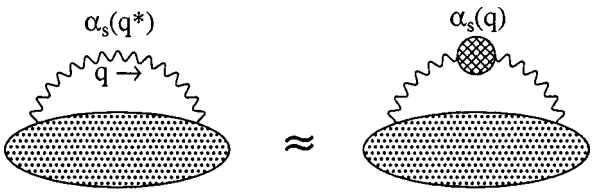

FIG. 1. The BLM prescription for fixing the optimum scale q^* to leading order in $\alpha_s(q^*)$.

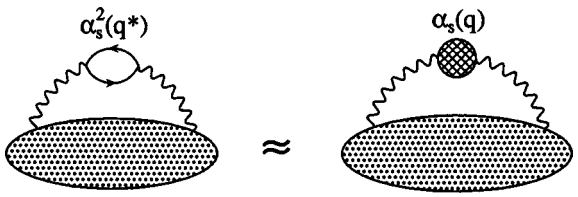

FIG. 2. The BLM prescription applied to a process for which a gluon contributes first at order $\alpha_s^2(q^*)$. The insertion on the left side represents vacuum polarization from both quarks and gluons.

flowing through its associated gluon. For a one-loop diagram with an integrand $f(q)$ which contributes predominantly at large gluon momentum q, a natural choice for the scale q^* of α_V is a mean value which reproduces the result of a fully dressed gluon within the diagram [4,13],

$$\alpha_V(q^*)\int d^4q f(q)=\int d^4q\,\alpha_V(q)f(q), \tag{1}$$

as illustrated in Fig. 1. However, $\alpha_V(q)$ possesses a pole at Λ_V, an artifact of an all-orders summation of perturbative logarithms. We avoid this singularity by truncating the series for $\alpha_V(q)$ at a finite order, as is appropriate for an asymptotic series.

Expanding $\alpha_V(q)$ in terms of $\alpha_V(q^*)$,

$$\begin{aligned}\alpha_V(q)&=\frac{\alpha_V(q^*)}{1+\alpha_V(q^*)\beta_0\log(q^2/q^{*2})}\\&\sim\alpha_V(q^*)-\alpha_V^2(q^*)\beta_0\log(q^2/q^{*2})+\cdots\end{aligned} \tag{2}$$

and solving to first nontrivial order gives [13]

$$\begin{aligned}\log(q^{*2})&=\frac{\int d^4q f(q)\log(q^2)}{\int d^4q f(q)}\equiv\frac{\langle f(q)\log(q^2)\rangle}{\langle f(q)\rangle}\\&\equiv\langle\langle\log(q^2)\rangle\rangle,\end{aligned} \tag{3}$$

a statement of this prescription suited for numerical calculations. Here

$$\beta_0\equiv\frac{1}{4\pi}\left(\frac{11}{3}C_A-\frac{4}{3}T_F n_f\right)=\frac{1}{4\pi}\left(11-\frac{2}{3}n_f\right), \tag{4}$$

and $\langle\langle\,\rangle\rangle$ indicates an average weighted by $f(q)$. For simplicity, we restrict the β function here to one loop, but show in Sec. VII that our result is not limited by this approximation.

By the definition of α_V, Eq. (3) guarantees that $\alpha_V(q^*)$ absorbs the effect of second-order vacuum polarization insertions in the gluon's propagator. An alternate method to determine q^* is then to require that β_0, or equivalently n_f, disappears to that order [4]. This version is useful when the β_0 or n_f dependence of coefficients in a perturbative expansion are known explicitly. We discuss this in more detail in Sec. V.

Equation (3) produces an optimum scale by means of an average of $\log(q^2)$ weighted by $f(q)$. As such, it provides a measure of the typical momentum carried by this gluon in the dominant integration region, in accord with intuition. However, in certain cases $\langle f\rangle$ vanishes, rendering q^* from Eq. (3) meaningless. This is a consequence of using an expression first order in $\alpha_V(q^*)$ for a process which is properly second order, rather than a flaw in the general prescription. When $\langle f\rangle$ vanishes, the diagram on the left in Fig. 1 does not contribute. The leading contribution from this gluon is second order, and the requirement that q^* be chosen to best approximate the all-order result leads to the equation illustrated in Fig. 2. For an integrand dominated by large momentum, the left side of Eq. (1) is replaced by

$$-\alpha_V^2(q^*)\beta_0\int d^4q f(q)\log(q^2/q^{*2}), \tag{5}$$

as is known from the running of $\alpha_V(q)$. Expanding $\alpha_V(q)$ as in Eq. (2) yields

$$\log(q^{*2})=\frac{\langle f\log^2(q^2)\rangle}{2\langle f\log(q^2)\rangle}. \tag{6}$$

This, rather than Eq. (3), is the appropriate statement of the prescription for this case.

As a simple illustration, consider a one-dimensional model for $f(q)$ in Eq. (1) for which the Feynman diagram produces an integrand with cancelling contributions

$$f(q)=\delta(q-q_a)-\delta(q-q_b); \tag{7}$$

here q_a and q_b are positive. Such cancellations are not uncommon in QCD for some choice of parameters, as for example in the calculations of Sec. IX B. A reasonable expectation would be that q^* should be some average of the contributing scales q_a and q_b, particularly if they are nearby. Because $\langle f\rangle$ vanishes identically, Eq. (3) produces a divergent q^*, whereas Eq. (6), which begins with the next order contribution, gives for q^* the more reasonable geometric mean

$$q^*=\sqrt{q_a q_b}. \tag{8}$$

This is the same scale obtained by Eq. (3) applied to the positive integrand

$$f(q)=\delta(q-q_a)+\delta(q-q_b), \tag{9}$$

as might be expected.

In other cases, while not strictly vanishing, $\langle f\rangle$ may be anomalously small, and the dominant contribution from this

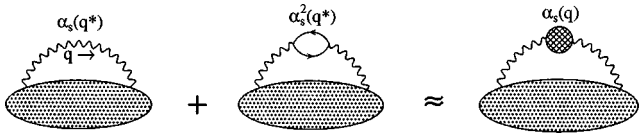

FIG. 3. The BLM prescription applied to second order in $\alpha_s(q^*)$. The insertion on the left side represents vacuum polarization from both quarks and gluons.

gluon is still as in Fig. 2. It is useful to generalize the lowest order prescription of Eq. (3) to incorporate both these cases naturally, and also to anticipate the situation where $\langle f\log(q^2)\rangle$ is anomalously small.

The discrepancy between the left and right sides of Eq. (1) relative to the lowest order term $\alpha_V(q^*)\int d^4q f(q)$ is

$$-\alpha_V(q^*)\beta_0\langle\langle\log(q^2/q^{*2})\rangle\rangle+\alpha_V^2(q^*)\beta_0^2\langle\langle\log^2(q^2/q^{*2})\rangle\rangle. \tag{10}$$

Applying Eq. (3) leaves a leading difference of

$$\alpha_V^2(q^*)\beta_0^2\langle\langle[\log(q^2)-\langle\langle\log(q^2)\rangle\rangle]^2\rangle\rangle\equiv\alpha_V^2(q^*)\beta_0^2\sigma^2 \tag{11}$$

with σ the standard deviation of $\log(q^2)$ with respect to the weight $f(q)/\langle f\rangle$. When $f(q)$ does not change sign, $f(q)/\langle f\rangle$ and σ^2 are both positive. When $f(q)$ changes sign and $\langle f\rangle$ is anomalously small due to cancellations, this error can become arbitrarily large, indicating that treating this as a first order process is invalid and it is useful to incorporate information from the next order.

Matching the gluon's contribution to next order to the fully dressed gluon, as in Fig. 3, adds the term in Eq. (5) to the left side of Eq. (1). Expanding both sides in terms of $\alpha_V(q^*)$ as before leads to a leading relative difference of

$$\begin{aligned}\alpha_V^2(q^*)\beta_0^2\langle\langle\log^2(q^2/q^{*2})\rangle\rangle&\\ =-\alpha_V^2(q^*)\beta_0^2[\log^2(q^{*2})-2\langle\langle\log(q^2)\rangle\rangle\log(q^{*2})&\\ +\langle\langle\log^2(q^2)\rangle\rangle].&\end{aligned} \tag{12}$$

When $f(q)/\langle f\rangle$ is positive for all q, this discrepancy is also strictly positive, and the best that can be done is to choose q^* to minimize it. The result of minimization is again just Eq. (3). This will also clearly be the case when $f(q)$ changes sign in some small region without significant cancellations. The leading error is then the same as in Eq. (11).

However, when $f(q)$ possesses significant sign changes, the error in Eq. (12) can become negative for certain values of $\log(q^{*2})$, and minimization is not appropriate. In this case, it is possible to eliminate the difference altogether by choosing one of the two solutions

$$\begin{aligned}\log(q^{*2})&=\frac{\langle f\log(q^2)\rangle\pm[\langle f\log(q^2)\rangle^2-\langle f\rangle\langle f\log^2(q^2)\rangle]^{1/2}}{\langle f\rangle}\\ &\equiv\langle\langle\log(q^2)\rangle\rangle\pm[\langle\langle\log(q^2)\rangle\rangle^2-\langle\langle\log^2(q^2)\rangle\rangle]^{1/2}\\ &\equiv\langle\langle\log(q^2)\rangle\rangle\pm[-\sigma^2]^{1/2}.\end{aligned} \tag{13}$$

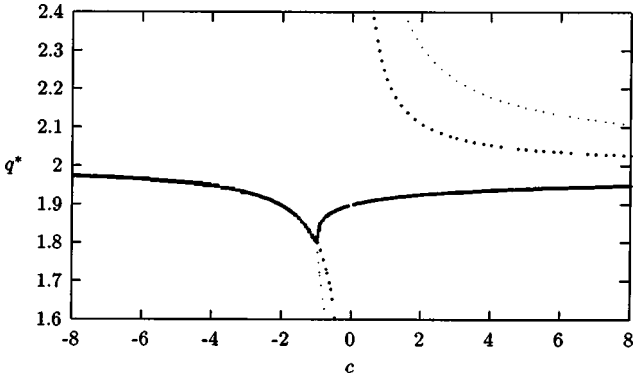

FIG. 4. The BLM scale q^* for the model of Eq. (14) as a function of c, with $q_a=2.0$ and $q_b=1.8$. The first order solution of Eq. (3) determines q^* for $c<-1$, the second order solution of Eq. (13) for $c>-1$. The dark dotted lines show the first-order solution in regions in which it does not apply; light dotted lines display inapplicable second-order solutions.

When the logarithmic moments are available over a range of parameters, requiring that q^* be continuous and physically sensible makes the proper choice apparent, as will be observed below. In particular, when $\langle f\rangle$ is nearly zero, this requires choosing the sign opposite to that of $\langle\langle\log(q^2)\rangle\rangle$. In every case we have considered, the choice has been obvious. However, if the need arises, one may resolve the sign unambiguously by using information from higher moments, as discussed in Sec. VII.

Were $f(q)$ a probability distribution, σ would be its standard deviation. A negative value for σ^2 indicates that $f(q)/\langle f\rangle$ has substantial changes of sign and is behaving significantly unlike a probability distribution. In this case, $\langle f\rangle$ will be anomalously small, the order $\alpha_V^2(q^*)$ contribution becomes important, and Eq. (13) provides the appropriate choice of scale. As a result, Eq. (13) determines q^* when σ^2 is negative, Eq. (3) when positive. This prescription is the main result of this paper.

Although Eq. (13) uses information from part of the next order, it is the appropriate scale to use when σ^2 is negative, even if only computing to first order in $\alpha_V(q^*)$. In that case, in addition to setting the scale for the leading term, it allows for a reasonable estimate of the magnitude of the neglected next-order terms, based on $\alpha_V^2(q^*)$. When $\langle f\rangle$ is very small, these neglected terms should give a sizable correction to the first-order term. And when one computes to order $\alpha_V^2(q^*)$ or higher using this scale, higher-order terms which dress the leading gluon should be small, having been largely absorbed into the first two, as in Fig. 3.

As an illustration, we consider a slightly more general version of the model of Eq. (7),

$$f(q)=(1+c)\,\delta(q-q_a)-\delta(q-q_b), \tag{14}$$

where $\langle f\rangle$ vanishes exactly for $c=0$, and has partial cancellation for $c>-1$. Figure 4 presents the scale q^* determined by Eq. (3) when $\sigma^2>0$ and by Eq. (13) when $\sigma^2<0$; that is, when $c>-1$. For $c<-1$, with no cancellations, Eq. (3) produces reasonable values for q^*. It falls between q_a and

q_b, approaching q_a for $|c|$ large, and q_b for $c=-1$. As c approaches zero and $\langle f\rangle$ vanishes, q^* from this prescription diverges. However, for $c>-1$, σ^2 is negative, and Eq. (13) provides the optimum scale. It evidently behaves according to expectations. Even for the case when c is large and positive and Eq. (3) produces a fairly sensible result, it overestimates q^* and Eq. (13) is preferable.

To summarize, we restate the prescription in a more compact form. We have chosen inclusion of the running coupling within the integrand for a first-order diagram, $\int d^4q\,\alpha_V(q)f(q)$, as a natural means to account for the running of the coupling with the gluon's momentum. It has the advantage that it incorporates higher-order diagrams which dress the gluon, has no arbitrary scale dependence, and appropriately accounts for the strength of the coupling of a gluon with momentum q.

It has the disadvantage that $\alpha_V(q)$ has an unphysical pole at $q=\Lambda_V$, making the integrand ill-defined. We avoid this by expanding $\alpha_V(q)$ at the scale q^* as in Eq. (2), and working to finite order in $\alpha_V(q^*)$, giving

$$\int d^4q f(q)[\alpha_V(q^*)-\beta_0\alpha_V^2(q^*)\log(q^2/q^{*2}) + \beta_0^2\alpha_V^3(q^*)\log^2(q^2/q^{*2})+\cdots]. \tag{15}$$

We choose q^* to reproduce the full integral as well as possible. In the absence of significant cancellations in $\int d^4q f(q)$, we may select the scale by Eq. (3) so that the first nonleading term in Eq. (15) vanishes. The discrepancy is then the term of order $\alpha_V^3(q^*)$, which this choice for q^* minimizes. Furthermore, as q^* will be near the typical q, $f(q)$ will be roughly even about q^*, and higher-order contributions should be either near zero or their minimum depending on whether they are even or odd in $\alpha_V(q^*)$.

However, when $f(q)$ is essentially odd about some q and so suffers from significant cancellations, this is not an appropriate prescription. The leading term in Eq. (15) will be anomalously small compared to the second term; in extreme cases, it might even vanish, and it would no longer make sense to absorb the second term into the leading term. Furthermore, the scale from Eq. (3) would no longer accurately represent the typical momentum, and neglected higher order terms in Eq. (15) would be anomalously large. It is, however, possible and sensible to require the third term to vanish by Eq. (6); that is, to absorb it into the first two. This again provides a typical scale about which, in this case, $f(q)$ is essentially odd, minimizes the fourth-order term, and suppresses higher-order terms.

III. SCHEMES OTHER THAN *V*

For prescriptions other than α_V, vacuum polarization insertions will in general contribute subleading constants in addition to terms as in Eq. (5). Though nonleading, these constants can make significant contributions at physically interesting values of q^2, and so the optimum scale ought to be chosen to account for them as well. One method for doing so is to focus on the fermion loop [4]. Both the $\log(q^2)$ and the subleading constant will appear multiplied by n_f. Replacing n_f with β_0 using Eq. (4) leaves the fermion loop contribution modified by a constant, to

$$-\alpha_s(q^*)\beta_0(\log(q^2/q^{*2})+a). \tag{16}$$

When applying the first-order prescription, amending Eq. (3) to

$$\log(q^{*2})=\langle\langle\log(q^2)+a\rangle\rangle \tag{17}$$

absorbs both the leading log and subleading constant into $\alpha_s(q^*)$. For the modified minimal subtraction scheme ($\overline{\rm MS}$), $a=-5/3$ [20–23], resulting in the shift in scale [4]

$$q^*_{\overline{\rm MS}}=\exp(-5/6)q^*_V=0.43q^*_V. \tag{18}$$

As with α_V, this also absorbs the log associated with gluon vacuum polarization, since β_0 determines its contribution relative to the fermion loop. However, the gluonic subleading constant need not contribute in this ratio, and so will not also be completely absorbed. One might choose instead to completely absorb the gluonic constant by solving Eq. (4) for the adjoint Casimir constant $C_A=N$ associated with the gluon loop in terms of β_0, before absorbing the β_0 term into $\alpha_s(q^*)$. This would be particularly appropriate when $n_f=0$, for example. For $\overline{\rm MS}$, the result is a factor of $\exp(-31/66)=0.63$, not greatly different from Eq. (18). This indicates that to one loop, absorbing the fermion loop constant also largely accounts for the gluonic constant.

When applying the second-order prescription, a constant subleading contribution leads to the same shift in Eq. (13) as in Eq. (17), with

$$\log(q^{*2})=\langle\langle\log(q^2)+a\rangle\rangle\pm[\langle\langle\log(q^2)\rangle\rangle^2 -\langle\langle\log^2(q^2)\rangle\rangle]^{1/2}. \tag{19}$$

The second term on the right is invariant under a shift in $\log(q^2)$ by a constant, and so remains unaffected.

Because the V scheme associates gluon exchange with a physical process at the specific scale q^{*2}, higher order contributions associated with the running of α_V must vanish identically when the gluon's momentum hits q^{*2}. As a result, logarithmic contributions $\log(q^2/q^{*2})$ from these diagrams appear without subleading constants.

IV. DETERMINING q^* IN $\overline{\rm MS}$

In order to provide a more realistic example, and to show how this prescription can be applied simply when using dimensional regularization, we determine q^* for the one-loop $g\phi^3$ diagram of Fig. 5. We intend this as a simplified version of a quark self-energy diagram, and employ it here for the sake of clarity.

By introducing an additional denominator of the form $(q^2)^\delta$ into this diagram in n-dimensional Euclidean space,

$$\frac{g^2}{2}\int\frac{d^nq}{(2\pi)^n}\,\frac{1}{q^2+m^2}\,\frac{1}{(p-q)^2+m^2}\,\frac{1}{(q^2)^\delta}, \tag{20}$$

and expanding the result in δ to second order, we produce the necessary logarithmic integrals:

$$\langle f(q)\rangle - \delta\langle f(q)\log(q^2)\rangle + \frac{\delta^2}{2}\langle f(q)\log^2(q^2)\rangle + \cdots. \tag{21}$$

(Note that Refs. [24,14] present a different and elegant technique for extracting these logarithmic moments based on a simple dispersion sum over a fictional gluon mass.)

We evaluate Eq. (20) using standard methods and obtain

$$\frac{g^2}{(4\pi)^2}\frac{\Gamma(\delta+\epsilon)}{\Gamma(\delta)}\int_0^1 dxdy y^{\delta-1}(1-y)\left[\frac{4\pi\mu^2}{M^2}\right]^{\epsilon}\left[\frac{1}{M^2}\right]^{\delta}, \tag{22}$$

where x and y are the usual Feynman parameters, $\epsilon \equiv (4-n)/2$, μ is introduced to keep g dimensionless, and

$$M^2 \equiv (1-y)m^2 + x(1-y)(1-x+xy)p^2. \tag{23}$$

The integration region $y \sim 0$ produces a $1/\delta$ singularity. Partial integration of $y^{\delta-1}$ makes this explicit, and allows us to expand in δ under the integral. Keeping terms in $1/\epsilon$ to order zero and comparing to Eq. (21) gives

$$\langle f(q)\rangle = -\frac{1}{\epsilon} + \int_0^1 dx \log\left(\frac{m^2+x(1-x)p^2}{\mu^2}\right) \tag{24}$$

$$\begin{aligned}\langle f(q)\log(q^2)\rangle = \int_0^1 dxdy\Bigg\{ &-\frac{1}{\epsilon^2} + \frac{1}{\epsilon}\log\left(\frac{y}{\mu^2}\right) + \frac{\pi^2}{12} \\ &- \frac{1}{2}\log^2\left(\frac{y}{\mu^2}\right) + \frac{1}{2}\log^2\left(\frac{M^2}{y}\right) \\ &+ \left[1 - \frac{x^2(1-y)^2p^2}{M^2}\right]\log\left(\frac{M^2}{y}\right)\Bigg\}\end{aligned} \tag{25}$$

$$\begin{aligned}\langle f(q)\log^2(q^2)\rangle = 2\int_0^1 dxdy\Bigg\{ &-\frac{1}{\epsilon^3} + \frac{1}{\epsilon^2}\log\left(\frac{y}{\mu^2}\right) \\ &+ \frac{1}{\epsilon}\left[\frac{\pi^2}{12} - \frac{1}{2}\log^2\left(\frac{y}{\mu^2}\right)\right] + \frac{1}{6}\Bigg[-\psi''(1) \\ &- \frac{\pi^2}{2}\log\left(\frac{y}{\mu^2}\right) + \log^3\left(\frac{y}{\mu^2}\right) \\ &+ 3\left[1 - \frac{x^2(1-y)^2p^2}{M^2}\right]\log^2\left(\frac{M^2}{y}\right) \\ &+ \log^3\left(\frac{M^2}{y}\right)\Bigg]\Bigg\}.\end{aligned} \tag{26}$$

In the above, we have dropped the overall factors $g^2/(4\pi)^2$, which are here irrelevant, and substituted $e^{\gamma}\mu^2/4\pi$ for μ^2. The latter greatly simplifies these expressions and allows us to apply the $\overline{\rm MS}$ prescription by subtracting the ϵ poles alone, as one would for MS.

To renormalize these terms, we note that the $\log(q^2)$ and $\log^2(q^2)$ factors integrated within this one-loop diagram stand in for the large-momentum contributions of the first two higher-order vacuum polarization subdiagrams which sum to form the running coupling. In particular, as these factors are finite, they represent these subdiagrams with their subdivergences already removed. For example, the factor $\log(q^2)$, which appears in the integrand which produced Eq. (25), comes from the large-momentum approximation to the $\overline{\rm MS}$-renormalized one-loop vacuum polarization diagram; that is, to Eq. (24) without the pole. The poles in ϵ which remain in Eqs. (24) to (26) are then the new overall divergences associated with one, two and three loops, respectively. In the $\overline{\rm MS}$ prescription these are simply discarded.

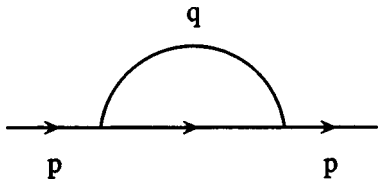

FIG. 5. One loop self-energy diagram in the $g\phi^3$ model.

Finally, we note that Eq. (24) in this model is the one-loop vacuum polarization diagram in addition to being the particle's self-energy. At large p^2, it is approximately $\log(p^2/\mu^2) - 2$, including the subleading constant. The constant a in Eq. (17) is then -2, and the $\overline{\rm MS}$ value for q^* will differ by a factor $\exp(-1)$ from the expression for q^* in the V scheme.

While Eqs. (24) to (26) allow us to determine q^* for any p and m, it is illuminating to consider two limits. When $p^2 \gg m^2$, after renormalization and choosing $\mu^2 = p^2$

$$\langle f(q)\rangle = -2 \tag{27}$$

$$\langle\langle \log(q^2)\rangle\rangle = \log(p^2) - \frac{\pi^2}{24} \tag{28}$$

$$\langle\langle \log^2(q^2)\rangle\rangle = \log^2(p^2) - \frac{\pi^2}{12}\log(p^2) + \left[\frac{\psi''(1)}{6} - \frac{\pi^2}{12} + 2\right] \tag{29}$$

to leading order in m^2/p^2. These give

$$\sigma^2 = 2 + \frac{\psi''(1)}{6} - \frac{\pi^2}{12}\left[1 + \frac{\pi^2}{48}\right]; \tag{30}$$

or numerically, $\sigma^2 = .6077$. The lowest order solution is then appropriate and yields a value for q^* close to p, with

$$q^*/p = \exp(-1)\exp(-\pi^2/48) = .2995, \tag{31}$$

which corresponds to a value of $\exp(-\pi^2/48) = .8141$ in the V scheme. We can use σ to give a measure of the relative spread in the momenta which contribute to this diagram, with

$$\Delta q/q \approx \sigma/2 = .3898, \tag{32}$$

independent of the prescription. In general, when $p^2 \gg m^2$ but for μ^2 arbitrary, $q^* \sim \sqrt{p\mu}$. This is the same result as Eq. (8), and reasonable for a diagram dominated by momenta between these two scales.

In the large mass limit $m \gg p$, with μ^2 chosen to equal the natural scale m^2, we find

$$\langle f(q) \rangle = \frac{1}{6} \frac{p^2}{m^2} \tag{33}$$

$$\langle f(q) \log(q^2) \rangle = \left(\frac{\pi^2 - 4}{4} \right) + \frac{1}{6} \log(m^2) \frac{p^2}{m^2} \tag{34}$$

$$\langle f(q) \log^2(q^2) \rangle = \left(\frac{\pi^2 - 4}{4} \right) [1 + \log(m^2)] - \frac{\psi''(1)}{3} + \frac{1}{3} \left[-1 + \frac{\pi^2}{6} + \frac{1}{2} \log^2(m^2) \right] \frac{p^2}{m^2} \tag{35}$$

to order p^2/m^2. Clearly in this limit $\langle f(q) \rangle$ becomes anomalously small, and we expect the second order solution to be necessary. We confirm this by noting that to this order

$$\langle f \rangle^2 \sigma^2 = -\left(\frac{\pi^2 - 4}{4} \right)^2 + \left[\left(\frac{\pi^2 - 4}{12} \right) - \frac{\psi''(1)}{18} \right] \frac{p^2}{m^2} \tag{36}$$

which is negative in this limit. The second order formula applies, and gives

$$\log(q^{*2}/m^2) = -2 + \left[1 - \frac{2\psi''(1)}{3(\pi^2 - 4)} \right] + \left[\frac{\pi^2 - 3}{9(\pi^2 - 4)} + \frac{4\psi''(1)}{27(\pi^2 - 4)^3} (-3(\pi^2 - 4) + \psi''(1)) \right] \frac{p^2}{m^2}, \tag{37}$$

or numerically,

$$q^*/m = 0.6953 + 0.0574 \; p^2/m^2. \tag{38}$$

For the V scheme, the leading -2 in Eq. (37) is absent, and

$$q_V^*/m = 1.8899 + 0.1562 \; p^2/m^2. \tag{39}$$

Figure 6 and Fig. 7 display q^* as a function of p for the respective cases where $\mu = p$ and $\mu = m$. The limiting values discussed above are evident. For $\mu = p$, the first-order solution determines q^* in both the large and small p regions, connected by the second-order solution in the interim. Immediately to the right of the point where the first-order solution diverges in Fig. 6, indicated by the vertical line, the second-order solution with positive root determines q^*; to the left, the second-order negative root applies. For $\mu = m$ (Fig. 7), the first-order solution applies for large p, the negative root second-order solution for small p. In both cases, use of the appropriate second order solution where applicable gives a meaningful and continuous value for q^* over the entire region in p. Which second-order solution to choose from Eq. (13) is obvious.

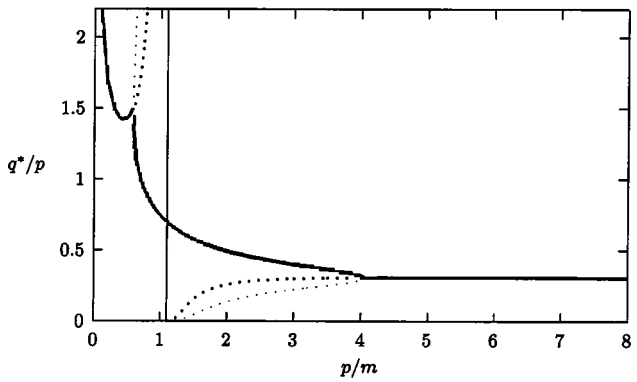

FIG. 6. The $\overline{\text{MS}}$ BLM scale q^*/p as a function of momentum p/m for the diagram of Fig. 5 in the scalar ϕ^3 model, with $\mu = p$. The first-order solution determines q^* in both the large and small p regions, connected by the second-order solution in the interim. The vertical line indicates the point where the first-order solution diverges. The dark dotted lines show the first-order solution in the region in which it does not apply; light dotted lines display inapplicable second-order solutions.

Finally, we note that computing higher order average logs for this diagram requires only expanding Eq. (22) to higher orders in δ, without the need to compute additional diagrams.

V. DETERMINING q^* FROM A KNOWN SERIES

To apply this prescription we need the first two logarithmic moments within the integrand associated with a gluon's propagator. Under certain conditions, we may apply this prescription to set the scale for a process for which the expansion is already known by examining its n_f dependence. At each order of $\alpha_V(\mu)$, the contribution from vacuum polarization will give the largest power of n_f, or equivalently, of β_0 [14,16,10]. It is therefore possible to read off the logarithmic integrals directly from the series coefficients.

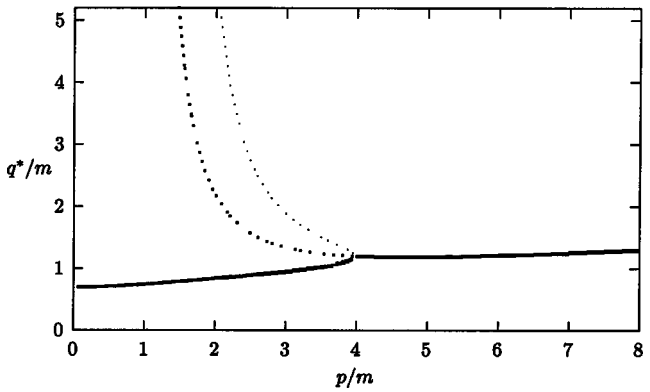

FIG. 7. The $\overline{\text{MS}}$ BLM scale q^*/m as a function of momentum p/m for the diagram of Fig. 5 in the scalar ϕ^3 model, with $\mu = m$. The first-order solution determines q^* in the large p region, while the negative root second-order solution gives q^* for small p. The dark dotted line shows the first-order solution in the region in which it does not apply; the light dotted line displays the inapplicable second-order solution.

Using Eq. (4) to replace the largest-n_f terms with β_0 in contributions associated with a particular gluon, we obtain a series of the form

$$c_0\alpha_V(\mu)+(a_1-c_1\beta_0)\alpha_V^2(\mu) +(a_2+\cdots+c_2\beta_0^2)\alpha_V^3(\mu)+\cdots. \tag{40}$$

The coefficients c_n are then associated with vacuum insertions in the gluon propagator. Comparison with the right sides of Eqs. (1) and (2) gives

$$\begin{aligned} c_0&=\langle f\rangle \\ c_1/c_0&\approx\langle\langle\log(q^2/\mu^2)\rangle\rangle \\ c_2/c_0&\approx\langle\langle\log^2(q^2/\mu^2)\rangle\rangle, \end{aligned} \tag{41}$$

which holds when $f(q)$ contributes predominantly at large q. Given this association, the prescription to second order is

$$\log(q^{*2}/\mu^2)=c_1/c_0\pm[(c_1/c_0)^2-c_2/c_0]^{1/2} \tag{42}$$

when the argument of the square root is positive, and

$$\log(q^{*2}/\mu^2)=c_1/c_0 \tag{43}$$

otherwise.

For schemes other than V, the presence of a subleading constant a contribution to fermion vacuum polarization leads to the identification

$$\begin{aligned} c_1/c_0&\approx\langle\langle\log(q^2/\mu^2)+a\rangle\rangle \\ c_2/c_0&\approx\langle\langle(\log(q^2/\mu^2)+a)^2\rangle\rangle. \end{aligned} \tag{44}$$

Because c_1 includes a and the square root is insensitive to it, Eq. (43) and Eq. (42) automatically incorporate the shift in Eq. (17) and so may be used unchanged. Also, if one is able to identify in the series the constants C_A associated with gluonic vacuum polarization, one could choose to use this instead to rewrite the series in terms of β_0. Equation (43) and Eq. (42) would then automatically absorb the subleading gluonic constant, as discussed at the end of Sec. II.

VI. COMBINING SERIES

Determining the scale for the series formed by multiplying two series,

$$F_a=1+c_a\alpha_V(q_a^*)+\cdots \tag{45}$$

and

$$F_b=1+c_b\alpha_V(q_b^*)+\cdots \tag{46}$$

with known scales is straightforward when considering only first-order scale setting:

$$F_{ab}\equiv F_aF_b=1+(c_a+c_b)\alpha_V(q_{ab}^*)+\cdots \tag{47}$$

with

$$\log(q_{ab}^{*2})=\frac{c_a\log(q_a^{*2})+c_b\log(q_b^{*2})}{c_a+c_b}. \tag{48}$$

Because of the need to first test the sign of the new σ_{ab}^2, the prescription for applying second-order scale setting is slightly more involved. In that case,

$$\begin{aligned} \sigma_{ab}^2&=\frac{c_a\langle\langle\log^2(q^2)\rangle\rangle_a+c_b\langle\langle\log^2(q^2)\rangle\rangle_b}{c_a+c_b} \\ &\quad-\left(\frac{c_a\langle\langle\log(q^2)\rangle\rangle_a+c_b\langle\langle\log(q^2)\rangle\rangle_b}{c_a+c_b}\right)^2 \\ &=\frac{c_a\sigma_a^2+c_b\sigma_b^2}{c_a+c_b}+\frac{c_ac_b}{(c_a+c_b)^2}(\langle\langle\log(q^2)\rangle\rangle_a \\ &\quad-\langle\langle\log(q^2)\rangle\rangle_b)^2. \end{aligned} \tag{49}$$

As usual, if $\sigma_{ab}^2>0$, the first order combination

$$\log(q_{ab}^{*2})=\frac{c_a\langle\langle\log(q^2)\rangle\rangle_a+c_b\langle\langle\log(q^2)\rangle\rangle_b}{c_a+c_b} \tag{50}$$

applies. If $\sigma_{ab}^2<0$,

$$\log(q_{ab}^{*2})=\frac{c_a\langle\langle\log(q^2)\rangle\rangle_a+c_b\langle\langle\log(q^2)\rangle\rangle_b}{c_a+c_b}\pm[-\sigma_{ab}^2]^{1/2}. \tag{51}$$

When combining two series by division, $F_{a/b}\equiv F_a/F_b$, the first-order coefficients subtract rather than add. The above formulas again apply, but with the replacement $c_b\to -c_b$. These also apply to series combined by addition and subtraction, respectively, because the results at first order are equivalent.

For schemes other than V, one should amend the average logs to include the subleading constants, as discussed in Sec. III. The relation between the scale in V and in other schemes remains the same.

VII. HIGHER ORDERS

Extending this prescription beyond second order is relatively straightforward, though it requires computation of $\langle\langle\log^3(q^2)\rangle\rangle$ and higher moments, or information from third-order and higher terms in a known series. An extension to third order, for example, would be necessary should both $\langle f\rangle$ and $\langle f\log(q^2)\rangle$ vanish, making the third term in Eq. (15) the leading term. Absorbing the subsequent term by requiring $\langle f\log^3(q^2/q^{*2})\rangle$ to vanish would give

$$\log(q^{*2})=\frac{\langle f\log^3(q^2)\rangle}{3\langle f\log^2(q^2)\rangle}, \tag{52}$$

as one would also obtain from Fig. 2 with two loops on the left side.

When $\langle f\rangle$ and $\langle f\log(q^2)\rangle$ are not identically zero but are anomalously small relative to higher moments, requiring $\langle f\log^3(q^2/q^{*2})\rangle$ to vanish still gives the appropriate scale. A

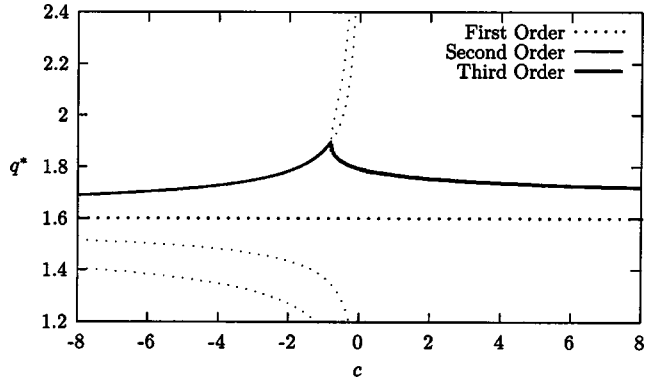

FIG. 8. The BLM scale q^* for the model of Eq. (53) as a function of c, with $q_a=2.0$, $q_b=1.8$ and $q_d=1.6$. The second-order solution determines q^* for $c<-1$, the third-order solution for $c>-1$. The dark dotted line shows the first-order solution; light dotted lines display inapplicable second and third-order solutions.

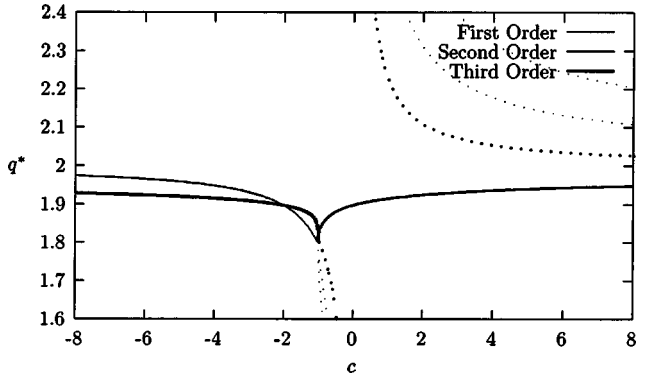

FIG. 9. The BLM scale for the δ-function model of Eq. (14) as in Fig. 4, but with the inclusion of the third-order solution. It is applicable for $c<-1$ and indicated by the additional dark line. Dotted lines indicate inapplicable solutions.

symptom that this is the case would be a third-order scale near Eq. (52) which shifts significantly the scale obtained at lower order, and which is more in line with physical expectations. If available, higher even moments near their minima or odd moments near zero at this scale would confirm it.

An order-n equation is necessary to set q^* only when all of the first $(n-2)$ moments vanish or are anomalously small. It would be unusual for a generic integrand $f(q)$ to be effectively orthogonal to more than a few powers of $\log(q^2)$, and so the need to use a high-order equation should be rare. We have found no realistic cases for which either Eqs. (3) or (13) were not sufficient.

In Fig. 8 we illustrate the appropriate scales for a model,

$$f(q)=A\,\delta(q-q_a)+B\,\delta(q-q_b)+(D+c)\,\delta(q-q_d), \tag{53}$$

with

$$B=-A\log(q_a/q_d)/\log(q_b/q_d), D=-(A+B), \tag{54}$$

contrived such that both $\langle f\rangle$ and $\langle f\log(q^2)\rangle$ vanish at $c=0$. The second- and third-order solutions behave as expected where appropriate; the first-order solution, while not divergent, is low throughout. The unphysical behavior of the first-order solution, as well as the significant discrepancy between first- and third-order scales indicate that the first-order result is inadequate.

Note the one- and two-node structures of the integrand $f(q)$ in the two- and three-delta models of Eq. (14) and Eq. (53), similar to generic first and second excited-state wave functions. This is the result of choosing $f(q)$ to be orthogonal to the zeroth, and to both the zeroth and first powers of $\log(q^2)$, respectively. Integrands requiring higher-order equations would necessarily have more nodes and additional detailed structure.

In general, higher-order solutions can confirm that a scale determined at a lower order is indeed typical. For example, in Fig. 9 we include the third order solution for the Eq. (14) model; where applicable, it does not differ significantly from the first-order result. This will also be apparent when we examine higher moments for certain processes in Sec. IX.

Thus far, for simplicity, we have restricted our discussion to contributions to $\alpha_V(q)$ from one loop vacuum polarization. We show here that the above expressions for q^* are not limited to these. Specifically, including subleading contributions to $\alpha_V(q)$ expanded within a diagram as in Eq. (15) gives

$$\begin{aligned}\alpha_V(q^*)\langle f\rangle &+ \alpha_V^2(q^*)[\beta_0\Delta_1]+\alpha_V^3(q^*)[\beta_0^2\Delta_2+\beta_1\Delta_1]\\ &+\alpha_V^4(q^*)\left[\beta_0^3\Delta_3+\frac{5}{2}\beta_0\beta_1\Delta_2+\beta_2\Delta_1\right]+\alpha_V^5(q^*)\\ &\times\left[\beta_0^4\Delta_4+\frac{13}{3}\beta_0^2\beta_1\Delta_3+3\beta_0\beta_2\Delta_2+\frac{3}{2}\beta_1^2\Delta_2+\beta_3\Delta_1\right]\\ &+\cdots.\end{aligned} \tag{55}$$

Here

$$\beta_1\equiv\frac{1}{(4\pi)^2}\left(102-\frac{38}{3}n_f\right), \tag{56}$$

and

$$\beta_2\equiv\frac{1}{(4\pi)^3}\left(\frac{2857}{2}-\frac{5033}{18}n_f+\frac{325}{58}n_f^2\right), \tag{57}$$

and we have defined the moments

$$\Delta_n\equiv\langle f\log^n(q^{*2}/q^2)\rangle=\langle f[\log(q^{*2})-\log(q^2)]^n\rangle. \tag{58}$$

We see from Eq. (55) that the reasoning which led to the prescriptions in Eq. (3) and Eq. (13) was not dependent on the leading-log approximation to $\alpha_V(q)$: the diagrams in each new set introduced by increasing the order of the leading-log approximation have as coefficients the same sequence of moments Δ_n as in the leading approximation. For nonanomalous cases, requiring Δ_1 to vanish via Eq. (3) absorbs the first leading-log correction, proportional to $\beta_0\Delta_1$, into the first term. It also absorbs the first next-to-leading log contribution, proportional to $\beta_1\Delta_1$, and so on for each loga-

rithmic order. And in each order, it leaves a leading discrepancy proportional to the moment Δ_2, which is minimized by Eq. (3). Insofar as this q^* represents the typical momentum carried by this gluon, higher-order terms proportional to higher moments should be suppressed. As a result, the first term $\alpha_V(q^*)\langle f\rangle$, with the choice of a single scale for q^*, should do reasonably well at approximating the right side of Eq. (1) regardless of the number of loops kept in the β function for $\alpha_V(q)$. When $\langle f\rangle$ vanishes or is anomalously small, it is inappropriate to absorb the leading correction at each logarithmic order into the vanishing or small first term. In this case Eq. (13) gives the appropriate scale. It causes Δ_2 to vanish, and so absorbs the second correction at each logarithmic order into the set of leading corrections. Again, because Eq. (13) produces a typical scale, higher-order terms should be small.

This illustrates one of the advantages of using a coupling based on a physical process, such as α_V. For other schemes, there can be significant subleading constants associated with the diagrams which dress the gluon, not accounted for in the running coupling. These will appear, for example, in the coefficients associated with the leading log term at each order n; that is, with β_0^{n-1}, as

$$\Delta_n \equiv \langle f[\log(q^{*2}) - (\log(q^2) + a_0)]^n \rangle, \tag{59}$$

and one may absorb them by adjusting the scale. However, only one such constant can be absorbed in this manner; parts of those associated with β_1 and higher will remain. By its definition, these constants cannot appear for α_V, and $\alpha_V(q^*)$ well represents the strength of a physical gluon at the scale q^*. This optimum choice of scale minimizes all coefficients associated with dressing the gluon, not just those associated with β_0.

VIII. IMPROVING CONVERGENCE

Thus far we have been considering the appropriate scale q^* for the leading α_V. For the sake of simplicity, we will be content to optimize the scale for the leading term, and will use the same scale for higher-order diagrams. From the previous discussion, it is clear that this will be a reasonable scale for diagrams which dress the leading-order gluon; these contributions should be small, having been largely absorbed into the leading term or terms. There is no reason to believe, however, that it will be the best scale for other higher-order diagrams, and it should certainly be possible to improve the convergence of the series by choosing the scale for such diagrams separately [4,10].

There are other cases for which it could prove advantageous to allow different scales at different orders, for different diagrams within the same order, or even within a single diagram. Returning to the simple and unexceptional model of Eq. (9), for which the first-order scale setting Eq. (3) gives Eq. (8), we note that the moments

$$\langle\langle \log^n(q^{*2}/q^2)\rangle\rangle = \frac{1}{2}[\log^n(q^{*2}/q_a^2) + \log^n(q^{*2}/q_b^2)] \tag{60}$$

become zero for n odd, and $\log^n(q_a/q_b)$ for n even. The latter grow in magnitude when the q_a is a few times greater than q_b. As these are proportional to the coefficients of terms which dress the gluon, terms in the series become ≈ 1 when this range q_a/q_b exceeds a few over α_s. The series becomes badly behaved then not only when the scale for α_s is low, but also when the range of important momenta is large [14,16].

Nevertheless, in this simple case the remedy is obvious. The problem results from requiring α_s at a single scale to incorporate two widely different scales. Separating these and writing the series for this model in terms of both $\alpha_s(q_a)$ and $\alpha_s(q_b)$ incorporates vacuum polarization contributions exactly and causes higher moments to vanish. This reinforces the idea that for a series in which gluons from different diagrams occur in loops sensitive to significantly different momenta, allowing the α_s associated with each to have its own scale could improve the series' convergence. Furthermore, for a series in which a gluon in a single diagram is sensitive to a wide range of momenta one might even consider improving its behavior by splitting up the integrand, with α_s at a different scale assigned to each region, as in the example above.

Even for diagrams which dress a specific gluon, it is possible to minimize higher moments by allowing the scale associated with these diagrams to differ at different orders. In particular, one may select the scale at every other order such that the following moment vanishes, and the next is minimized. Variations in the scale would account for the different regions the moments probe in the integrand.

We will not pursue this further here, but mention that care must be taken to preserve gauge invariance if separate scales are assigned to different parts of a series.

IX. APPLICATIONS

A. Known series

In Table I we present a collection of results for perturbative quantities for which at least the second logarithmic moment is available, allowing us to apply scale setting beyond lowest order. Reference [10] presents a useful compilation and discussion of many of these. These include the log of the 1×1 Wilson loop in lattice QCD ($-\log W_{11}$) [13,25], the ratio of e^+e^- goes to hadrons over muons ($R_{e^+e^-}$) [26–30], the ratio of the quark pole mass to its $\overline{\rm MS}$ mass ($M/\overline{M}$) [31–36] and [14,16], the ratio of τ goes to ν_τ + hadrons over τ goes to $\nu_\tau e^- \overline{\nu}_e$ (R_τ) [37–42] and [29,30,15], the semileptonic B-meson decay width ($\Gamma(B\to X_u e\overline{\nu})$) [43–50] expressed both in terms of the pole and $\overline{\rm MS}$ b-quark masses, the top quark decay width ($\Gamma(t\to bW)$) [51–56] and [24,46,14] in terms of its pole and $\overline{\rm MS}$ masses, the Bjorken sum rules for polarized electroproduction ($\int_0^1 dx[g_1^{\rm ep}(x,Q^2) - g_1^{\rm en}(x,Q^2)]$) [57–62], and deeply inelastic neutrino-nucleon scattering ($\int_0^1 dx[F_1^{\nu{\rm p}}(x,Q^2) - F_1^{\nu{\rm p}}(x,Q^2)]$) [63–66], and the static quark potential ($V(Q^2)$) [20–23] and [67,68].

We note that the nonsinglet part of the Ellis-Jaffe sum rule [69–72] and [62] gives the same scale as the former Bjorken

TABLE I. Applications of second-order scale setting to several processes. The coefficients c_n are defined in Sec. V. q_1^* gives the scale set by Eq. (3). q_2^* gives the preferred scale by Eq. (13) where appropriate, also indicated by boxes. Δq measures the range of momentum running through the gluon.

c_1/c_0	q_1^*	c_2/c_0	σ^2	q_2^*	Δq
$-\log W_{11}$:					
2.448	$3.402/a$	6.316	0.3194	–	$0.96/a$
$R_{e^+e^-}(s)$:					
−0.691772	$0.7076\sqrt{s}$	−0.186421	−0.66497	$\boxed{1.064\sqrt{s}}$	–
$M/\bar{M}$:					
−4.6862	$0.09603M$	17.623	−4.3374	$\boxed{0.27205M}$	$0.38M$
R_τ:					
−2.2751	$0.32060M_\tau$	5.6848	0.50872	–	$0.11M_\tau$
$\Gamma(B\to X_u e\bar{\nu})/M_b^5$:					
−5.3382	$0.06932M_b$	34.410	5.9139	–	$0.084M_b$
$\Gamma(B\to X_u e\bar{\nu})/\bar{M}_b^5$:					
−4.3163	$0.11554M_b$	8.0992	−10.531	$\boxed{0.58534M_b}$	$0.35M_b$
$\Gamma(t\to bW)/M_t^3$:					
−4.2054	$0.12213M_t$	23.046	5.3611	–	$0.14M_t$
$\Gamma(t\to bW)/\bar{M}_t^3$:					
−5.7076	$0.05763M_t$	6.0996	−26.477	$\boxed{0.75502M_t}$	$0.34M_t$
$\int_0^1 dx[g_1^{ep}(x,Q^2)-g_1^{en}(x,Q^2)]$:					
−2	$e^{-1}Q=0.3679Q$	115/18	43/18	–	$0.28Q$
$\int_0^1 dx[F_1^{\bar{\nu}p}(x,Q^2)-F_1^{\nu p}(x,Q^2)]$:					
−8/3	$e^{-4/3}Q=0.2636Q$	155/18	3/2	–	$0.16Q$
$V(Q^2)$:					
−5/3	$e^{-5/6}Q=0.4346Q$	25/9	0	–	0

sum rule, the Gross-Llewellyn Smith sum rule [73,64,61,62] the same scale as the latter.

All but the first scales are from known $\overline{\text{MS}}$ series, and for these at least the fermion vacuum polarization graphs must be given to two loops. In several cases higher logarithmic moments are known, which will allow us to test the consistency of the procedure. We find four cases where the second-order formula gives the preferred scale.

When the first-order solution is appropriate, the second moment gives a rough measure of the range in momenta which flow through the gluon, with

$$\frac{\Delta q}{q}\approx\frac{1}{2}\left(\frac{\Delta_2}{\langle f\rangle}\right)^{1/2}. \tag{61}$$

Here, Δq is the standard deviation in q and Δ_2 is defined in Eq. (58). A large range results in large coefficients at higher orders, as discussed above, and may indicate sensitivity to low q. When the second-order scale is appropriate, Eq. (61) clearly is not. However, if higher moments are available, we may estimate this range using

$$\frac{\Delta q}{q}\approx\left|\frac{\Delta_{n+2}}{4(n+1)\Delta_n}\right|^{1/2}, \tag{62}$$

with n odd. In Table I, we use $n=1$. This expression gives the standard deviation in a distribution modeled by a Gaussian times $[\log(q^{*2})-\log(q^2)]^n$ to render it odd. We found it to give reasonably consistent results for various n when applied to several examples discussed below, though other measures are certainly possible.

For $R_{e^+e^-}$, $M/\bar{M}$, and both $\Gamma(B\to X_u e\bar{\nu})$ and $\Gamma(t\to bW)$ expressed in terms of $\overline{\text{MS}}$ masses, we find that the second-order scale is appropriate, leading to significant corrections to the anomalously low first-order scales, especially in the latter three. While the new scale for $M/\bar{M}$ is significantly increased, we note that $\Delta q/q$ is still relatively large, indicating sensitivity to low-momentum scales even when M is large, and threatening a poorly behaved series. This apparently infects the b and t decay rates when expressed in terms of pole masses, as shown by their low scales. By contrast, $\overline{\text{MS}}$ masses behave more as bare masses, being sensitive to short distances; expressing the two decays in terms of these

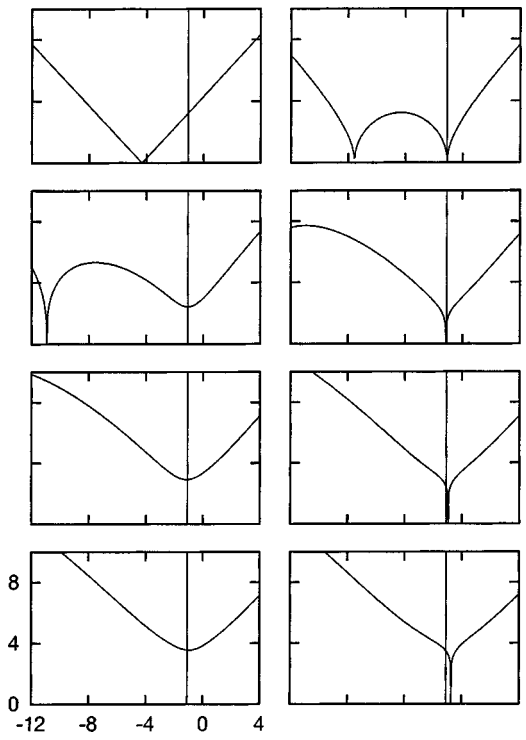

FIG. 10. The moments $|\langle\langle[\log(q^{*2}_{\overline{\rm MS}})-\log(q^2)]^n\rangle\rangle|^{1/n}$ as functions of $\log(q^{*2}_{\overline{\rm MS}}/M_b^2)$ for $n=1$ to 8 (left to right) for $\Gamma(B\to X_u e\overline{\nu}_e)$ over the $\overline{\rm MS}$ mass $\overline{M}_b$. The vertical line indicates the choice for the scale $\log(q^{*2}_{\overline{\rm MS}}/M_b^2)$ using Eq. (13). By choosing the second-order prescription such that the second moment vanishes, $\log(q^{*2}_{\overline{\rm MS}}/M_b^2)$ is either near the minimum or the zero for all higher moments, minimizing higher-order terms in Eq. (55).

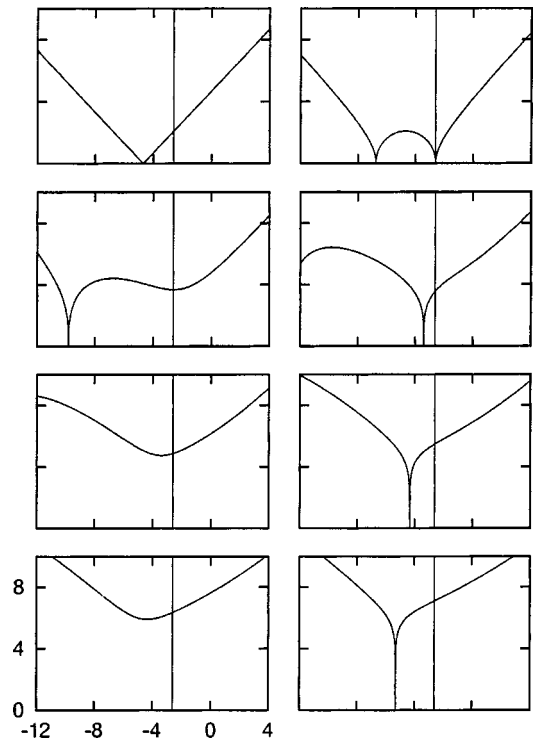

FIG. 11. The moments $|\langle\langle[\log(q^{*2}_{\overline{\rm MS}})-\log(q^2)]^n\rangle\rangle|^{1/n}$ as functions of $\log(q^{*2}_{\overline{\rm MS}}/M^2)$ for $n=1$ to 8 (left to right) for $M/\overline{M}$. The vertical line indicates the choice for the scale $\log(q^{*2}_{\overline{\rm MS}}/M^2)$ using Eq. (13).

significantly improves their behavior [55,74,24,14,15]. This is clear from both their scales and widths. Both these series should be well-behaved, and well-represented by α_s at a single, physically reasonable scale. But it is necessary to use second-order scale setting to see this; the first-order q^* for each indicates a scale which is misleadingly low.

References [14,15,47] provide very useful values for fermion vacuum polarization contributions, and therefore logarithmic moments, computed to eighth order for the pole to $\overline{\rm MS}$ ratio, τ, B and t decays. These allow us to compute their Δq's using Eq. (62), but more importantly, to confirm the general picture as discussed in Sec. VII. In Fig. 10 we use this information to display the first eight moments $|\langle\langle[\log(q^{*2}_{\overline{\rm MS}})-\log(q^2)]^n\rangle\rangle|^{1/n}$ as functions of $\log(q^{*2}_{\overline{\rm MS}}/M_b^2)$ for $\Gamma(B\to X_u e\overline{\nu}_e)$ expressed in terms of the $\overline{\rm MS}$ mass $\overline{M}_b$. Here $q^{*2}_{\overline{\rm MS}}$ absorbs the fermion loop constant associated with the $\overline{\rm MS}$ prescription, as in Eq. (18), and M_b is the b-quark pole mass. We observe that choosing $\log(q^{*2}_{\overline{\rm MS}}/M_b^2)$ to set the second moment to zero using Eq. (13) not only removes it and minimizes the third moment, it also sets all of the higher moments near their minima or zeros. It is clear that this is the natural scale for this process, and that terms beyond second order which dress the leading gluon should be small. The first moment is clearly anomalous, and setting it to zero using Eq. (3) would evidently lead to large higher-order corrections. In general, we expect $f(q)$ to be either roughly even or odd about its typical scale q^*, and the sign of the second moment, σ^2, should distinguish the two. For Δq sufficiently small, using Eq. (3) or Eq. (13) depending on the sign of σ^2 should give reasonable values except in very rare cases.

The picture for $M/\overline{M}$, Fig. 11, is similar. While choosing the second order scale is more appropriate than first, causing the second moment to vanish and minimizing the third, the zeros and minima of higher moments drift progressively lower. Such behavior is anticipated by the relatively large value of $\Delta q/q$, which indicates a wide range of contributing momenta. In this case, higher moments are increasingly sensitive to lower q, and the corresponding coefficients will progressively increase. We might improve the convergence of the series by methods discussed in Sec. VIII. For example, choosing q^* separately at each odd order in α_s, causing the following even moment to vanish and miminizing the subsequent odd moment, with each q^* indicating the characteristic scale for that moment. An alternative is to resum the entire set of polarization diagrams [14,16]. Regardless, the ability to detect sensitivity to a large range of momenta, in addition to the scale itself, by computing the first few logarithmic moments is sufficient to warn of large higher order corrections. In this case, it suggests using $\overline{M}$ rather than M in expressions for b and t decays.

B. Quark mass and energy renormalization in lattice NRQCD

Lattice nonrelativistic QCD (NRQCD) is an effective field theory designed to reproduce the results of continuum QCD

TABLE II. The BLM scale for the pole mass renormalization factor Z_m for several values of the bare lattice mass aM_0 in NRQCD without tadpole improvement. aq_1^* gives the scale set by Eq. (3) in units of the inverse lattice spacing. aq_2^* gives the preferred scale by Eq. (13) where appropriate. The parameter n is set to ensure the stability of heavy quark propagator evolution in simulations [76].

n	aM_0	$\langle f\rangle\equiv(Z_m-1)/\alpha_s$	$\langle f\log((aq)^2)\rangle$	$\langle f\log^2((aq)^2)\rangle$	aq_1^*	aq_2^*
1	20.00	0.4679(39)	1.343(11)	4.091(62)	4.202(71)	–
	17.50	0.4860(34)	1.364(10)	4.196(65)	4.068(58)	–
	15.00	0.5125(30)	1.3907(85)	4.211(41)	3.883(44)	–
	12.50	0.5410(46)	1.426(14)	4.242(63)	3.736(65)	–
	10.00	0.5880(35)	1.463(12)	4.384(68)	3.469(43)	–
	7.00	0.7057(17)	1.5423(58)	4.880(32)	2.982(15)	–
	5.00	0.8624(14)	1.7153(48)	5.538(29)	2.7034(87)	–
	4.00	1.0071(27)	1.9021(70)	6.062(32)	2.571(11)	–
2	4.00	1.0177(23)	1.9264(80)	6.164(33)	2.577(11)	–
	3.50	1.1268(23)	2.0710(83)	6.614(53)	2.507(10)	–
	3.00	1.2853(21)	2.2859(68)	7.351(35)	2.4333(74)	–
	2.70	1.4119(19)	2.4540(79)	7.911(34)	2.3846(73)	–
	2.50	1.5188(23)	2.6141(74)	8.390(52)	2.3646(66)	–
	2.00	1.9018(22)	3.1745(79)	10.214(32)	2.3039(53)	–
	1.70	2.2751(24)	3.7546(75)	12.039(56)	2.2823(43)	–
	1.60	2.4384(24)	4.0086(79)	12.857(39)	2.2750(41)	–
	1.50	2.6320(22)	4.3141(78)	13.745(37)	2.2694(37)	–
3	1.40	2.8804(23)	4.7587(76)	15.073(37)	2.2842(34)	–
	1.20	3.5010(22)	5.7986(83)	18.143(39)	2.2891(30)	–
	1.00	4.4915(19)	7.4780(68)	23.109(31)	2.2990(19)	–
5	0.80	6.3033(34)	10.720(11)	32.131(63)	2.3405(24)	–

TABLE III. The BLM scale for the pole mass renormalization factor Z_m for several values of the bare lattice mass aM_0 in NRQCD with tadpole improvement. aq_1^* gives the scale set by Eq. (3) in units of the inverse lattice spacing. aq_2^* gives the preferred scale by Eq. (13) where appropriate. The parameter n is set to ensure the stability of heavy quark propagator evolution in simulations [76].

n	aM_0	$\langle f\rangle\equiv(Z_m-1)/\alpha_s$	$\langle f\log((aq)^2)\rangle$	$\langle f\log^2((aq)^2)\rangle$	aq_1^*	aq_2^*
1	20.00	−0.2381(39)	−0.385(11)	−0.367(62)	2.246(61)	1.34(11)
	17.50	−0.2224(34)	−0.371(10)	−0.278(65)	2.301(60)	1.240(91)
	15.00	−0.1996(30)	−0.3530(85)	−0.286(41)	2.422(61)	1.262(73)
	12.50	−0.1773(46)	−0.333(14)	−0.293(63)	2.56(12)	1.29(13)
	10.00	−0.1416(35)	−0.323(12)	−0.223(68)	3.14(16)	1.21(12)
	7.00	−0.0566(17)	−0.3242(58)	0.066(32)	17.6(1.7)	0.95(13)
	5.00	0.0386(14)	−0.3018(48)	0.335(29)	0.0201(31)	0.75(17)
	4.00	0.1126(27)	−0.2881(70)	0.413(32)	0.278(12)	0.650(59)
2	4.00	0.1232(23)	−0.2638(80)	0.515(33)	0.343(13)	0.471(81)
	3.50	0.1722(23)	−0.2664(83)	0.586(53)	0.461(12)	–
	3.00	0.2381(21)	−0.2783(68)	0.737(35)	0.5574(85)	–
	2.70	0.2828(19)	−0.3107(79)	0.781(34)	0.5773(84)	–
	2.50	0.3180(23)	−0.3261(74)	0.807(52)	0.5988(74)	–
	2.00	0.4183(22)	−0.4581(79)	0.846(32)	0.5783(57)	–
	1.70	0.4899(24)	−0.6166(75)	0.765(56)	0.5329(44)	0.57(12)
	1.60	0.5131(24)	−0.7058(79)	0.699(39)	0.5027(42)	0.723(23)
	1.50	0.5376(22)	−0.8143(78)	0.518(37)	0.4689(37)	0.835(17)
3	1.40	0.5795(23)	−0.8755(76)	0.542(37)	0.4698(34)	0.839(15)
	1.20	0.6212(22)	−1.2529(83)	−0.043(39)	0.3648(28)	1.009(13)
	1.00	0.6518(19)	−1.9239(68)	−1.139(31)	0.2286(16)	1.152(11)
5	0.80	0.6964(34)	−3.009(11)	−3.277(63)	0.1153(15)	1.293(24)

TABLE IV. The BLM scale for the energy shift E_0 for several values of the bare lattice mass aM_0 in NRQCD without tadpole improvement. aq_1^* gives the scale set by Eq. (3) in units of the inverse lattice spacing. aq_2^* gives the preferred scale by Eq. (13) where appropriate. The parameter n is set to ensure the stability of heavy quark propagator evolution in simulations [76].

n	aM_0	$\langle f\rangle \equiv E_0/\alpha_s$	$\langle f\log((aq)^2)\rangle$	$\langle f\log^2((aq)^2)\rangle$	aq_1^*	aq_2^*
1	20.00	2.25711(48)	2.5490(13)	10.8100(38)	1.75884(55)	–
	17.50	2.27657(44)	2.6011(12)	10.9496(40)	1.77051(52)	–
	15.00	2.30333(45)	2.6694(13)	11.1328(39)	1.78507(54)	–
	12.50	2.33892(69)	2.7653(22)	11.3882(87)	1.80606(92)	–
	10.00	2.39196(65)	2.9062(23)	11.7729(84)	1.83583(92)	–
	7.00	2.50419(41)	3.1988(14)	12.5623(49)	1.89398(57)	–
	5.00	2.64980(48)	3.5784(15)	13.5643(49)	1.96446(59)	–
	4.00	2.77360(93)	3.8995(38)	14.4035(99)	2.0198(15)	–
2	4.00	2.77159(78)	3.8981(28)	14.380(11)	2.0203(11)	–
	3.50	2.8585(10)	4.1118(34)	14.952(11)	2.0529(13)	–
	3.00	2.97012(88)	4.3973(34)	15.670(12)	2.0965(13)	–
	2.70	3.0574(11)	4.6137(38)	16.228(11)	2.1266(15)	–
	2.50	3.12485(90)	4.7822(41)	16.660(12)	2.1494(15)	–
	2.00	3.3492(12)	5.3483(43)	18.116(15)	2.2221(16)	–
	1.70	3.5394(13)	5.8316(43)	19.302(14)	2.2791(15)	–
	1.60	3.6163(13)	6.0299(45)	19.843(16)	2.3018(16)	–
	1.50	3.7057(14)	6.2486(45)	20.406(17)	2.3236(16)	–
3	1.40	3.7865(16)	6.4417(61)	20.873(18)	2.3411(21)	–
	1.20	4.0175(17)	7.0245(61)	22.344(17)	2.3970(20)	–
	1.00	4.32658(96)	7.8282(35)	24.418(11)	2.4711(11)	–
5	0.80	4.6581(20)	8.7418(74)	26.784(27)	2.5557(23)	–

TABLE V. The BLM scale for the energy shift E_0 for several values of the bare lattice mass aM_0 in NRQCD with tadpole improvement. aq_1^* gives the scale set by Eq. (3) in units of the inverse lattice spacing. aq_2^* gives the preferred scale by Eq. (13) where appropriate. The parameter n is set to ensure the stability of heavy quark propagator evolution in simulations [76].

n	aM_0	$\langle f\rangle \equiv E_0/\alpha_s$	$\langle f\log((aq)^2)\rangle$	$\langle f\log^2((aq)^2)\rangle$	aq_1^*	aq_2^*
1	20.00	1.05283(48)	−0.3998(13)	3.2048(38)	0.82706(52)	–
	17.50	1.04985(44)	−0.4027(12)	3.2027(40)	0.82549(50)	–
	15.00	1.04669(45)	−0.4076(13)	3.1970(39)	0.82306(51)	–
	12.50	1.04040(69)	−0.4143(22)	3.1878(87)	0.81948(89)	–
	10.00	1.03060(65)	−0.4272(23)	3.1758(84)	0.81281(90)	–
	7.00	1.00820(41)	−0.4643(14)	3.1150(49)	0.79431(56)	–
	5.00	0.97428(48)	−0.5243(15)	2.9833(49)	0.76409(58)	–
	4.00	0.94100(93)	−0.5878(38)	2.8305(99)	0.7318(15)	–
2	4.00	0.93900(78)	−0.5891(28)	2.807(11)	0.7307(11)	–
	3.50	0.9137(10)	−0.6502(34)	2.671(11)	0.7006(13)	–
	3.00	0.87572(88)	−0.7311(34)	2.444(12)	0.6588(13)	–
	2.70	0.8466(11)	−0.7996(38)	2.266(11)	0.6236(15)	–
	2.50	0.82102(90)	−0.8590(41)	2.111(12)	0.5927(15)	–
	2.00	0.7312(12)	−1.0621(43)	1.583(15)	0.4837(16)	–
	1.70	0.6442(13)	−1.2576(43)	1.018(14)	0.3768(15)	0.7950(59)
	1.60	0.6056(13)	−1.3421(45)	0.830(16)	0.3302(14)	0.8460(65)
	1.50	0.5641(14)	−1.4439(45)	0.566(17)	0.2781(14)	0.9029(73)
3	1.40	0.4953(16)	−1.6171(61)	0.088(18)	0.1955(16)	0.986(12)
	1.20	0.3523(17)	−1.9501(61)	−0.802(17)	0.06282(99)	1.106(24)
	1.00	0.13779(96)	−2.4285(35)	−2.035(11)	0.0001489(93)	1.23(11)
5	0.80	−0.3161(20)	−3.4380(74)	−4.629(27)	230.0(8.4)	1.416(75)

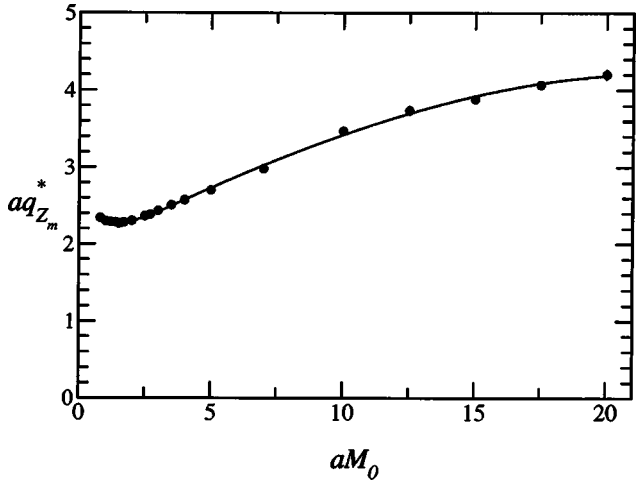

FIG. 12. The BLM scale q^* for the pole mass renormalization factor Z_m as a function of the bare lattice mass aM_0 in NRQCD without tadpole improvement. The first order solution determines q^* for all values.

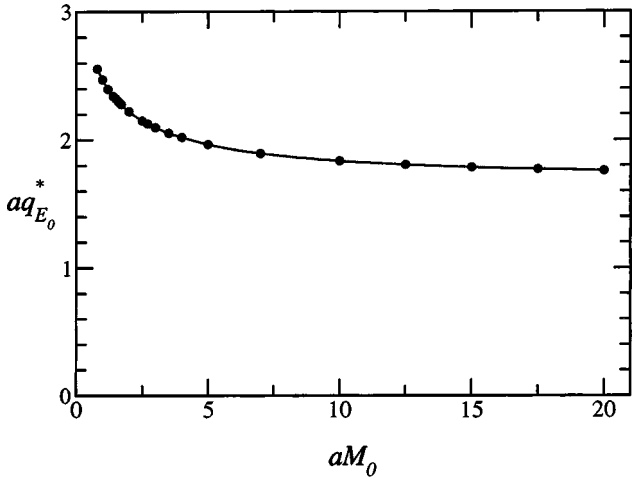

FIG. 14. The BLM scale q^* for the energy shift E_0 as a function of bare lattice mass aM_0 in NRQCD without tadpole improvement. The first order solution determines q^* for all values.

for a heavy quark at energies small relative to its mass [75–77]. Higher-dimensional operators provide systematic corrections ordered by quark velocity v and lattice spacing a, and account for radiative processes above the cutoff, typically around the mass. For a cutoff much larger than $\Lambda_{\rm QCD}$, lattice perturbation theory should give reliable values for the coefficients of these operators as well as the renormalization factors which connect bare to physical quantities. Reference [13] demonstrates that this expectation is valid, provided one uses a renormalized rather than bare coupling constant, and divides link gauge fields by their mean value to remove large tadpole contributions peculiar to the lattice.

References [78–80] present calculations of two of these quantities to first order in α_s: the renormalization factor Z_m, which connects the bare lattice heavy quark mass to its pole mass, and E_0, the shift from zero of the nonrelativistic energy of a heavy quark at rest. Reference [80], using an action improved to Ov^2 and Oa^2, and to $\mathcal{O}v^4$ for spin-dependent interactions, found that first-order scale setting produced anomalous results for certain values of the bare mass, particularly after tadpole improvement.

In Tables II–V and Figs. 12–15, we present new values for the scale for a variety of bare quark masses M_0, both with and without tadpole improvement. By applying Eq. (13) in regions where appropriate, we obtain a reasonable scale for all values of M_0, correcting the anomalies observed in Ref. [80]. As expected, there is a significant reduction in the scale after tadpole improvement. The tadpole contributions to these renormalizations are quadratically divergent in the inverse lattice spacing, and so are generally large and sensi-

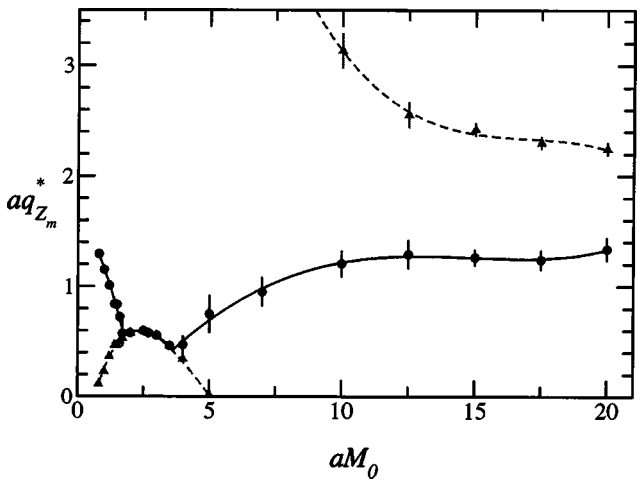

FIG. 13. The BLM scale q^* for the pole mass renormalization factor Z_m as a function of the bare lattice mass aM_0 in NRQCD with tadpole improvement. The first order solution determines q^* between $aM_0=2.00$ and 3.50, the second order elsewhere. Circles indicate the appropriate scale; triangles indicate the first-order solution in regions where it does not apply.

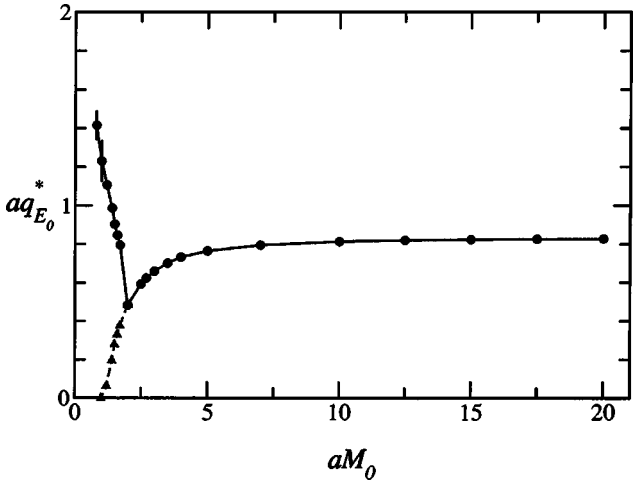

FIG. 15. The BLM scale q^* for the energy shift E_0 as a function of bare lattice of the bare lattice mass aM_0 in NRQCD with tadpole improvement. The first order solution determines q^* between $aM_0=0.80$ and 1.70, the second order elsewhere. Circles indicate the appropriate scale; triangles indicate the first-order solution in regions where it does not apply.

tive to large momenta. Tadpole improvement is designed to remove the bulk of these contributions, and so reduces the typical scale from 2–4 to 0.5–1.5 in units of the inverse lattice spacing a.

X. CONCLUSIONS

In this paper we have derived a method which incorporates information from higher orders into the general prescription of Ref. [4] for choosing the optimal scale q^* for the strong coupling constant α_s. We find that it corrects erroneous scales where the leading term or terms are anomalously small.

The extended prescription states that Eq. (13) determines the optimal scale q^* when the argument of the square root is positive. When it is not, the first order formula in Eq. (3) applies. The choice of sign for the second-order solution should be apparent either from continuity, or by checking that the solution minimizes the next higher (cubic) moment in Eq. (55) if it is available. In addition, higher moments give a measure of the range Δq of momenta which flow through the gluon, and can confirm that the q^* chosen in either case is indeed typical. Large values for the relative range $\Delta q/q$ can indicate large higher-order contributions even when q^* is large.

Our second-order prescription has several advantages. It requires a simple extension to the calculation, either numeric and analytic, needed to implement the first-order prescription, requiring only computation of an additional logarithmic moment. Calculation of higher moments can then help to further characterize the diagram and confirm the scale choice. It can also identify cases where the first two terms are anomalously small, though such cases are apparently rare. It is appropriate regardless of the number of loops included in the running coupling. Finally, it remedies erroneous scales in a variety of processes.

ACKNOWLEDGMENTS

We are grateful to S. Brodsky, C. Davies and J. Shigemitsu for helpful conversations. K.H. thanks the members of the Newman Laboratory theory group, Cornell, for their hospitality. This work was supported in part by grants from the National Science Foundation and the Department of Energy.

[1] P.M. Stevenson, Phys. Lett. **100B**, 61 (1981); Phys. Rev. D **23**, 2916 (1981); Nucl. Phys. **B203**, 472 (1982); **B231**, 65 (1984).
[2] G. Grunberg, Phys. Lett. **95B**, 70 (1980); Phys. Rev. D **29**, 2315 (1984).
[3] J. Kubo and S. Sakakibara, Z. Phys. C **14**, 345 (1982).
[4] S.J. Brodsky, G.P. Lepage, and P.B. Mackenzie, Phys. Rev. D **28**, 228 (1983).
[5] A. Dhar and V. Gupta, Phys. Rev. D **29**, 2822 (1984).
[6] V.V. Starshenko and R.N. Faustov, Dubna Jinr-N7-85 (85, REC. MAY), pp. 39–44.
[7] V. Gupta, D.V. Shirkov, and O.V. Tarasov, Int. J. Mod. Phys. A **6**, 3381 (1991).
[8] H.J. Lu, Phys. Rev. D **45**, 1217 (1992).
[9] H. Lu and S.J. Brodsky, Phys. Rev. D **48**, 3310 (1993).
[10] S.J. Brodsky and H.J. Lu, Phys. Rev. D **51**, 3652 (1995).
[11] S.J. Brodsky, E. Gardi, G. Grunberg, and J. Rathsman, Phys. Rev. D **63**, 094017 (2001).
[12] G. Grunberg and A.L. Kataev, Phys. Lett. B **279**, 352 (1992).
[13] G.P. Lepage and P.B. Mackenzie, Phys. Rev. D **48**, 2250 (1993).
[14] M. Beneke and V.M. Braun, Phys. Lett. B **348**, 513 (1995).
[15] P. Ball, M. Beneke, and V.M. Braun, Nucl. Phys. **B452**, 563 (1995).
[16] M. Neubert, Phys. Rev. D **51**, 5924 (1995).
[17] S.J. Brodsky, J. Ellis, E. Gardi, M. Karliner, and M.A. Samuel, Phys. Rev. D **56**, 6980 (1997).
[18] A.X. El-Khadra, Nucl. Phys. B (Proc. Suppl.) **34**, 141 (1994).
[19] C.T.H. Davies, K. Hornbostel, G.P. Lepage, A. Lidsey, J. Shigemitsu, and J. Sloan, Phys. Lett. B **345**, 42 (1995); C.T.H. Davies, K. Hornbostel, G.P. Lepage, P. McCallum, J. Shigemitsu, and J. Sloan, Phys. Rev. D **56**, 2755 (1997).
[20] L. Susskind, in *Weak and Electromagnetic Interactions At High Energies*, Les Houches, 1976, Proceedings (North-Holland, Amsterdam, 1977), pp. 207–308.
[21] W. Fischler, Nucl. Phys. **B129**, 157 (1977).
[22] A. Billoire, Phys. Lett. **92B**, 343 (1980).
[23] W. Buchmüller, G. Grunberg, and S.-H.H. Tye, Phys. Rev. Lett. **45**, 103 (1980); **45**, 587(E) (1980).
[24] B.H. Smith and M.B. Voloshin, Phys. Lett. B **340**, 176 (1994).
[25] T.R. Klassen, Phys. Rev. D **51**, 5130 (1995)
[26] K.G. Chetyrkin, A.L. Kataev, and F.V. Tkachev, Phys. Lett. **85B**, 277 (1979).
[27] M. Dine and J. Sapirstein, Phys. Rev. Lett. **43**, 668 (1979).
[28] W. Celmaster and R.J. Gonsalves, Phys. Rev. Lett. **44**, 560 (1980).
[29] S.G. Gorishnii, A.L. Kataev, and S.A. Larin, Phys. Lett. B **259**, 144 (1991).
[30] L.R. Surguladze and M.A. Samuel, Phys. Rev. Lett. **66**, 560 (1991).
[31] R. Tarrach, Nucl. Phys. **B183**, 384 (1981).
[32] N. Gray, D.J. Broadhurst, W. Grafe, and K. Schilcher, Z. Phys. C **48**, 673 (1990).
[33] D.J. Broadhurst, N. Gray, and K. Schilcher, Z. Phys. C **52**, 111 (1991).
[34] J. Fleischer, F. Jegerlehner, O.V. Tarasov, and O.L. Veretin, Nucl. Phys. **B539**, 671 (1999).
[35] K.G. Chetyrkin and M. Steinhauser, Nucl. Phys. **B573**, 617 (2000).
[36] K. Melnikov and T.v. Ritbergen, Phys. Lett. B **482**, 99 (2000).
[37] E. Braaten, Phys. Rev. Lett. **60**, 1606 (1988).
[38] E. Braaten, Phys. Rev. D **39**, 1458 (1989).
[39] S. Narison and A. Pich, Phys. Lett. B **211**, 183 (1988).
[40] E. Braaten, S. Narison, and A. Pich, Nucl. Phys. **B373**, 581 (1992).
[41] F. Le Diberder and A. Pich, Phys. Lett. B **286**, 147 (1992).
[42] A.A. Pivovarov, Z. Phys. C **53**, 461 (1992).

[43] S.M. Berman, Phys. Rev. **112**, 267 (1958).
[44] T. Kinoshita and A. Sirlin, Phys. Rev. **113**, 1652 (1959).
[45] Y. Nir, Phys. Lett. B **221**, 184 (1989).
[46] M. Jezabek and J.H. Kuhn, Nucl. Phys. **B314**, 1 (1989).
[47] P. Ball, M. Beneke, and V.M. Braun, Phys. Rev. D **52**, 3929 (1995).
[48] M. Luke, M.J. Savage, and M.B. Wise, Phys. Lett. B **343**, 329 (1995).
[49] M. Luke, M.J. Savage, and M.B. Wise, Phys. Lett. B **345**, 301 (1995).
[50] T. van Ritbergen, Phys. Lett. B **454**, 353 (1999).
[51] N. Cabibbo, G. Corbo, and L. Maiani, Nucl. Phys. **B155**, 93 (1979).
[52] M. Jezabek and J.H. Kuhn, Phys. Lett. B **207**, 91 (1988).
[53] M. Jezabek and J.H. Kuhn, Nucl. Phys. **B320**, 20 (1989).
[54] C.S. Li, R.J. Oakes, and T.C. Yuan, Phys. Rev. D **43**, 3759 (1991).
[55] B.H. Smith and M.B. Voloshin, Phys. Rev. D **51**, 5251 (1995).
[56] A. Czarnecki, Acta Phys. Pol. **26**, 845 (1995).
[57] J.D. Bjorken, Phys. Rev. **148**, 1467 (1966).
[58] J.D. Bjorken, Phys. Rev. D **1**, 1376 (1970).
[59] J. Kodaira, S. Matsuda, T. Muta, K. Sasaki, and T. Uematsu, Phys. Rev. D **20**, 627 (1979).
[60] J. Kodaira, S. Matsuda, K. Sasaki, and T. Uematsu, Nucl. Phys. **B159**, 99 (1979).
[61] S.G. Gorishnii and S.A. Larin, Phys. Lett. B **172**, 109 (1986).
[62] S.A. Larin and J.A. Vermaseren, Phys. Lett. B **259**, 345 (1991).
[63] J.D. Bjorken, Phys. Rev. **163**, 1767 (1967).
[64] W.A. Bardeen, A.J. Buras, D.W. Duke, and T. Muta, Phys. Rev. D **18**, 3998 (1978).
[65] S.G. Gorishnii, S.A. Larin, F.V. Tkachev, and K.G. Chetyrkin, Phys. Lett. **137B**, 230 (1984).
[66] S.A. Larin, F.V. Tkachev, and J.A. Vermaseren, Phys. Rev. Lett. **66**, 862 (1991).
[67] M. Peter, Phys. Rev. Lett. **78**, 602 (1997); Nucl. Phys. **B501**, 471 (1997).
[68] Y. Schroder, Phys. Lett. B **447**, 321 (1999).
[69] J. Ellis and R. Jaffe, Phys. Rev. D **9**, 1444 (1974); **10**, 1669(E) (1974).
[70] J. Kodaira, Nucl. Phys. **B165**, 129 (1980).
[71] S.A. Larin, Phys. Lett. B **334**, 192 (1994).
[72] S.A. Larin, T. van Ritbergen, and J.A. Vermaseren, Phys. Lett. B **404**, 153 (1997).
[73] D.J. Gross and C.H. Lewellyn Smith, Nucl. Phys. **B14**, 337 (1969).
[74] I.I. Bigi, M.A. Shifman, N.G. Uraltsev, and A.I. Vainshtein, Phys. Rev. D **50**, 2234 (1994).
[75] W.E. Caswell and G.P. Lepage, Phys. Lett. **167B**, 437 (1986).
[76] B.A. Thacker and G.P. Lepage, Phys. Rev. D **43**, 196 (1991).
[77] G.P. Lepage, L. Magnea, C. Nakhleh, U. Magnea, and K. Hornbostel, Phys. Rev. D **46**, 4052 (1992).
[78] C.T. Davies and B.A. Thacker, Phys. Rev. D **45**, 915 (1992).
[79] C.J. Morningstar, Phys. Rev. D **48**, 2265 (1993).
[80] C.J. Morningstar, Phys. Rev. D **50**, 5902 (1994).